International Journal of Climatology

International Journal of Climatology | RMetS

RESEARCH ARTICLE

The Role of the Central American Monsoon in the Seasonal Variability of Tropical Cyclone Activity in the Western Hemisphere

Connor DeLaune[1,2] | Vasubandhu Misra[1,2] | C. B. Jayasankar[2]

[1]Department of Earth, Ocean and Atmospheric Science, Florida State University, Tallahassee, Florida, USA | [2]Center for Ocean-Atmospheric Prediction Studies, Florida State University, Tallahassee, Florida, USA

Correspondence: Vasubandhu Misra (vmisra@fsu.edu)

Received: 4 October 2025 | **Revised:** 25 December 2025 | **Accepted:** 20 January 2026

Keywords: central American monsoon | ENSO teleconnections | hurricanes | tropical cyclones | tropical easterly waves

ABSTRACT

The Central American Monsoon (CAM) is closely linked to the seasonal migration of the Intertropical Convergence Zone (ITCZ) during summer, and its onset is correlated with tropical cyclone (TC) activity in the western hemisphere, comprising the northern tropical eastern Pacific and the tropical Atlantic ocean basins. We find that an early (late) CAM onset is generally associated with reduced (enhanced) May–November TC activity in the eastern Pacific, but with increased (reduced) activity in the eastern Caribbean and western tropical North Atlantic. Similarly, variations in CAM onset are connected to changes in tropical easterly wave (TEW) activity, as identified from multiple reanalysis datasets. These relationships appear to be mediated through concurrent anomalies in mid-level relative humidity, vertical wind shear, sea surface temperatures (in the eastern Pacific) and North Atlantic subtropical high. We also evaluate the teleconnections of the Oceanic Niño Index (ONI), which represents ENSO variability, with seasonal TC activity in both basins. While the ONI exhibits a stronger and more direct influence on TC variability than CAM onset, the onset variations provide an important additional source of predictability. CAM onset leads the seasonal TC activity in the western hemisphere by 15–30 days, unlike ENSO, whose teleconnections are largely contemporaneous. Notably, the association between CAM onset and ONI is weak, suggesting that these drivers act partly independently. Our results indicate that CAM onset timing can modulate ENSO-related teleconnections, either reinforcing or offsetting them depending on ENSO phase. This highlights the role of CAM onset as a precursor for seasonal TC variability in the western hemisphere.

1 | Introduction

El Niño and the Southern Oscillation (ENSO) is one of the main sources of seasonal predictability of seasonal Tropical Cyclone (TC) activity in the western hemisphere that includes the oceanic basins of Tropical North Atlantic (TNA) and northern Tropical East Pacific (TEP; Gray 1984; Bell and Chelliah 2006; Camargo et al. 2008; Klotzbach 2011; Balaguru et al. 2013). Warm or cold ENSO events are known to be associated with weaker or stronger seasonal TC activity in the TNA basin, while stronger or weaker TC activity in the TEP basin respectively. This association stems from the implied modulation of the Walker Circulation by the evolution of ENSO. This modulation results in the associated changes to vertical wind shear, large-scale subsidence, mid-level relative humidity, large-scale atmospheric stability and disturbances such as Tropical Easterly Waves (TEWs) emanating from west Africa that affect the TC activity in the TNA (Goldenberg et al. 2001; Gray 1984; Klotzbach 2007; Ruti and Dell'Aquila 2010; Shapiro 1987; Tang and Neelin 2004; Vecchi and Soden 2007). Similarly, ENSO variations affect the SST anomalies, vertical wind shear and low-level vorticity from the variations in the ITCZ that affect the seasonal TC activity in the

TEP, along with the generation of TEWs in the TEP or their sustenance from the TNA (Camargo and Sobel 2005; Collins 2007; Frank and Young 2007; Klotzbach 2011).

In this study, we are examining an additional predictor of seasonal TC activity in the western hemisphere from the variations of the Central American Monsoon (CAM). CAM is regarded as the bridge between the North and the South American Monsoon (Vera et al. 2006). In a recent study, Rodgers et al. (2024) report the complex evolution of the CAM rainfall and show that the onset date of CAM relates very strongly to its seasonal length and rainfall. The study indicates that early or late onset compared to climatology is associated with longer and wetter or shorter and drier CAM season respectively. They used this local relationship to successfully demonstrate that a reliable seasonal outlook could be provided across Central America by monitoring the onset date of CAM. Other studies have suggested that variations of CAM are also associated with corresponding variability of the North Atlantic Subtropical High (NASH), SST variations and TEWs in the TNA (Durán-Quesada et al. 2017, 2020; Misra et al. 2014).

The relation of ENSO with CAM is complex. For instance, the ENSO impact on moisture transport and rainfall of CAM is different between its Caribbean and Pacific coasts (Amador, Rivera, et al. 2016; Durán-Quesada et al. 2020). Waylen et al. (1996) indicate that the orography of Central America on either side of the Central Cordillera constrains the ENSO teleconnections over CAM. Furthermore, ENSO teleconnection with CAM evolves over the season, with competing influence from TNA (Amador, Rivera, et al. 2016; Enfield and Alfaro 1999; Giannini et al. 2000). As a result, Rodgers et al. (2024) show that ENSO teleconnection on the total seasonal anomalies of CAM is obfuscated and appears insignificant. However, CAM seasonal rainfall displays significant interannual variability, strongly related to the local variations of the onset date of CAM (Rodgers et al. 2024). Therefore, it is worthwhile to examine the potential influence of CAM variations on the TC activity of the western hemisphere, as it could provide an additional source of predictability on seasonal TC activity in the western hemisphere from monitoring the onset date of CAM. Furthermore, it may be noted that the CAM onset occurs in the April/May timeframe, which is prior to the beginning of the TEP and TNA hurricane seasons, providing a natural lead time of 15 days to a month for seasonal predictions.

2 | Datasets and Methodology

The period of the analysis conducted in this study is from 1981 to 2023 (=43 years). The analysis is confined to the TC seasons for the TEP and the TNA from May to November. In this study, environmental variables analysed included winds at 850 and 200, 850 hPa geopotential heights and mid-level (700 hPa) relative humidity, from the European Center for Medium-Range Weather Forecasts ReAnalysis version 5 (ERA5; Hersbach et al. 2020). This is available on a monthly time scale on a 0.25°×0.25° grid. Similarly, NOAA OISSTv2 (Huang et al. 2021; Reynolds et al. 2007) was also used at the same temporal and spatial resolution from 1982 to 2023 as ERA5. We examine the variations of the basin-wide statistics of TCs in the TNA and TEP from Colorado State University (2025). We adopt partial correlations (Radok and Brown 1993) to isolate the influence of ENSO and CAM variations on the basin-wide TC metrics like Accumulated Cyclone Energy (ACE; the square of the maximum sustained winds at each 6-h fix integrated over the lifetime of each TC and for all TCs in the season), total number of tropical storms, hurricanes, major hurricanes, etc., and environmental parameters such as bulk wind shear, mid-level moisture and 850 hPa geopotential heights. Partial correlations reveal the correlation between the focal variables after removing the effect of the confounding variable. For example, the partial correlation between ENSO variations and total number of tropical storms in one of the basins is revealed after the impact of CAM variations on the total number of tropical storms is removed. The partial correlation ($r_{AB,C}$) is computed as:

$$r_{AB,C} = \frac{\left(r_{AB} - r_{AC}r_{BC}\right)}{\left(\sqrt{\left(1 - r_{AC}^2\right)} - \sqrt{\left(1 - r_{BC}^2\right)}\right)} \quad (1)$$

where $r_{AB,C}$ is the partial correlation between variables A and B after the effect of C is removed. Similarly, r_{AC}, r_{BC} in Equation (1) refers to correlations between variables A and C, and between B and C respectively.

The TEWs are identified at 600 hPa at 6-hourly intervals using an objective tracking algorithm following Belanger et al. (2017). This algorithm uses the advection of curvature vorticity anomalies derived from the 2-D wind field to track TEWs along with the following additional criteria applied at 600 hPa: (1) advection of curvature vorticity anomaly equalling 0 s^{-2}, (2) curvature vorticity anomaly exceeding the 66th percentile of all the anomalies, (3) zonal wind being less than 2.5 ms^{-1}, (4) median speed being between −25 m/s and −2 m/s to ensure westward propagation and (5) TEW lasting at least 2 days. The five different reanalyses utilised in this study include ERA5 (Hersbach et al. 2020), Climate Forecast System-Reanalysis (CFS-R; Saha et al. 2010), ECMWF Reanalysis Interim (ERA-Interim; Dee and Coauthors 2011) and ECMWF Reanalysis-40 (ERA-40; Uppala and Coauthors 2005) and National Centers for Environmental Prediction/National Center for Atmospheric Research Reanalysis (NCEP-NCAR; Kalnay and Coauthors 1996). The resolution and period of analysis for each dataset are listed in Table 1. NOAA HURDAT2 (Landsea and Franklin 2013) was utilised to determine the number and track densities of named storms.

We used the Oceanic Niño Index (ONI) metric for ENSO variations following Barnston et al. (1997). The ONI is seasonally averaged SST anomalies over the Niño3.4 region (5° N–5° S, 120°–170° W) in the eastern equatorial Pacific Ocean and is extensively utilised by NOAA's Climate Prediction Center for characterising ENSO variations (Huang et al. 2017; Webb and Magi Webb and Maggi 2022).

Following the methodology in Rodgers et al. (2024), we compute the onset date of CAM based on area-averaged rainfall over the terrestrial regions of Panama, Costa Rica and Nicaragua available from the high-resolution (0.05°×0.05°) daily Climate Hazards Group Infrared Precipitation with Station (CHIRPS; Funk et al. 2015) from 1981 to 2023. The

TABLE 1 | Spatial and temporal resolutions and periods of analysis for each dataset utilised in the TEW analysis.

Dataset	Spatial resolution	Temporal resolution	Period of analysis	References
ERA5	0.25°×0.25°	6 hourly	1986–2022	Hersbach et al. (Hersbach et al. 2020)
CFSR	0.5°×0.5°	6 hourly	1979–2010	Saha et al. (2010)
NCEP-NCAR	210×210 km	6 hourly	1974–2010	Kalnay et al. (1996)
ERA-Interim	1°×1°	6 hourly	1979–2010	Dee et al. (2011)
ERA-40	120×120 km	6 hourly	1965–2001	Uppala et al. (2005)

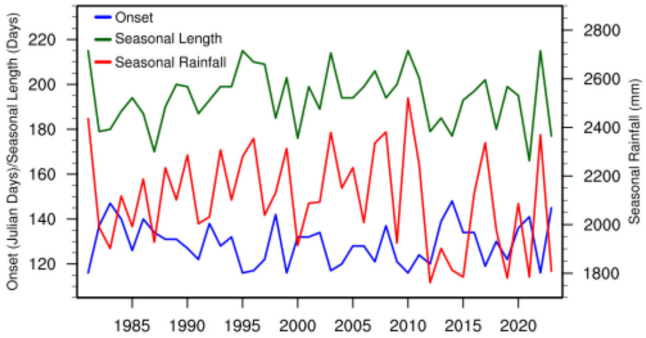

FIGURE 1 | The time series of the onset date, seasonal rainfall and seasonal length of the Central American Monsoon (CAM) averaged over Panama, Costa Rica and Nicaragua. The correlation between onset date and seasonal length is −0.75 and that between onset date and seasonal rainfall is −0.53. [Colour figure can be viewed at wileyonlinelibrary.com]

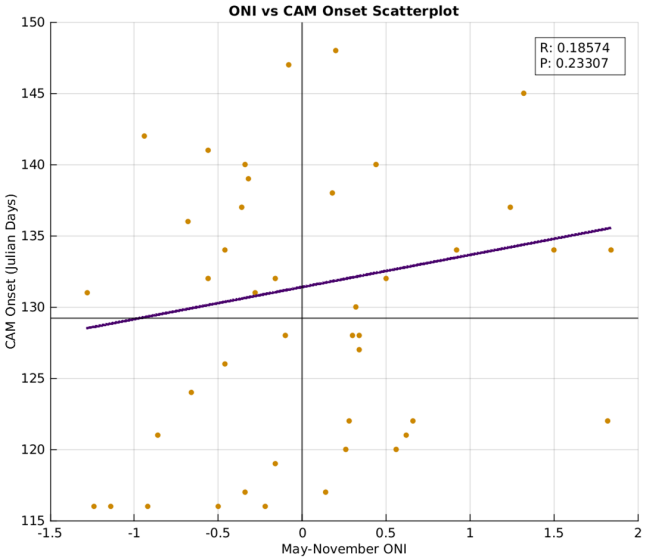

FIGURE 2 | The scatter between the Central American Monsoon (CAM) onset date (in Julian Days) and May to November averaged Oceanic Niño Index (ONI) with a fitted regression line. The corresponding correlation (R) and its *p* value (P) are indicated in the legend. [Colour figure can be viewed at wileyonlinelibrary.com]

onset date is objectively defined as the first day of the year when the daily rain rate exceeds the annual mean climatological rain rate. Instead of computing the local onset dates of CAM at every grid point as is done in Rodgers et al. (2024), we resorted to computing an area-averaged onset date to have a single index to represent CAM variations. We also restricted the area average to the southern half of the CAM region (including Panama, Costa Rica and Nicaragua) as it accounts for most of the seasonal rain of CAM and occurs slightly earlier than the northern half, which would present itself as a predictor with greater lead time for seasonal TC activity in the western hemisphere.

3 | Results

3.1 | The CAM Onset Date Variations

As noted earlier, the onset date of the CAM has a significant influence on the length of the CAM season and the seasonal rainfall (Rodgers et al. 2024). An early or a later onset of the CAM is associated with longer or shorter and a wetter or a drier CAM season respectively. This is demonstrated in Figure 1, which shows the time series of the onset date overlaid with the corresponding timeseries of the seasonal rainfall and seasonal length. The correlations of the timeseries of the onset date with the corresponding timeseries of seasonal rainfall and seasonal length in Figure 1 are −0.75 and −0.53 respectively.

The association of CAM onset date variations with ENSO variations is rather weak (Rodgers et al. 2024; Figure 2). Figure 2 shows a scatter between the ONI and onset date variations of CAM, which are weakly related to each other with a weak correlation of 0.19 and a *p* of 0.23. Rodgers et al. (2024) argue that the weak ENSO teleconnections in CAM variability—contrary to findings in other studies (e.g., Amador, Rivera, et al. 2016; Durán-Quesada et al. 2020)—arise from how the CAM season is defined. ENSO-related influences change over the course of the season: the early CAM period is more strongly linked to TNA variability, whereas the later period in the CAM season shows a clearer connection to ENSO (Amador 2008; Amador, Rivera, et al. 2016; Durán-Quesada et al. 2017; Enfield and Alfaro 1999; Giannini et al. 2000). Furthermore, Rodgers et al. (2024) report that other large-scale variations like the inter-basin SST gradient between the TNA and TEP, the Atlantic and the TEP warm pools, also show similar insignificant relationships with the onset date variations of CAM. Therefore, Rodgers et al. (2024) indicate that CAM onset date variations are largely dictated by local, internal variations and their strong relation to the CAM seasonal rainfall variability implies that it offers a stiff challenge to the seasonal predictability of the CAM rainfall. It should be noted that CAM onset dates that nominally occur between mid-April and mid-May offer a short lead time for the seasonal outlook of CAM, which was successfully

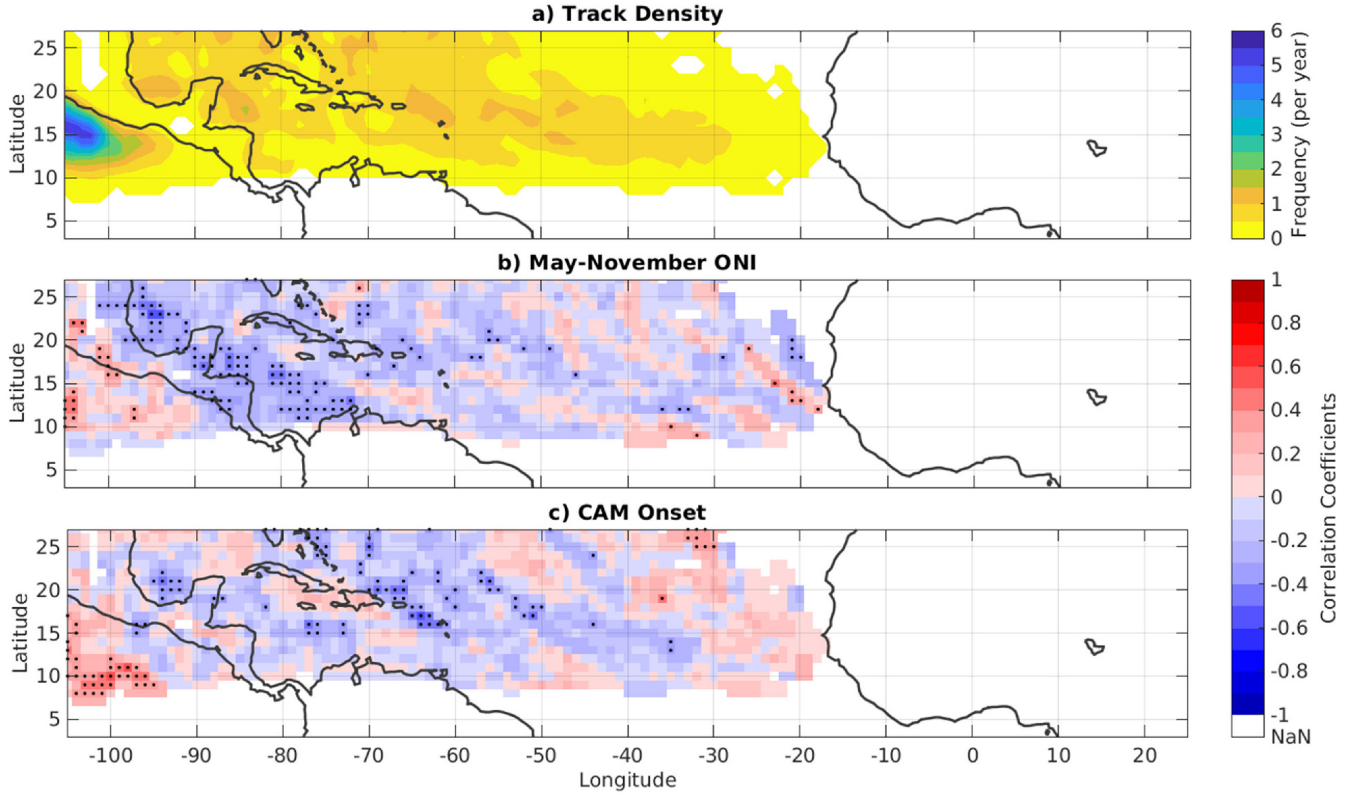

FIGURE 3 | (a) The climatology (1981–2023) of track density of all named May to November tropical cyclones from HURDAT2. The partial correlations of the track density of all May to November named tropical cyclones from HURDAT2 with (b) corresponding Oceanic Niño Index (ONI) and (c) Central American Monsoon (CAM) onset dates. The stippled values signify statistical significance at 5% significance level according to t-test. [Colour figure can be viewed at wileyonlinelibrary.com]

demonstrated in Rodgers et al. (2024). Likewise, we intend to utilise this lead time offered by the CAM onset date variations to understand its influence on TCs in the western hemisphere.

3.2 | Western Hemisphere Tropical Cyclone Activity Variability

Figure 3a shows the track density or number of TCs per 2°×2° grid per year of all named TCs in the TNA and TEP from HURDAT2 over the 1981–2023 period (43 years). The comparatively high density of TCs in the TEP (west of 90° W) in the domain is apparent (Figure 3a). The regions of high TC activity in the tropical Atlantic Ocean were captured in the western Caribbean region and in the Main Development Region (MDR), albeit less than that over TEP (Figure 3a). The corresponding correlations of this track density with ONI in Figure 3b suggest significant negative correlations in the Caribbean Sea, parts of the western Atlantic Ocean, the western Gulf of Mexico, along the Caribbean coast of Central America and Pacific coast of Nicaragua. This teleconnection suggests that positive or negative ONI, meaning El Niño or La Niña conditions, are related to weaker or stronger TC activity over these regions in the TNA respectively. Similarly, in Figure 3b we observe positive correlations of the ONI with track density in the TEP and along Pacific coasts of Mexico and Guatemala, which suggests increased or decreased TC activity with El Niño or La Niña conditions respectively. These correlations over TEP are less spatially extensive than in TNA (Figure 3b).

TABLE 2 | Partial correlations of basin-wide tropical cyclone metrics for northern tropical Atlantic Ocean.

Basin-wide metric	CAM onset date variations		ENSO variations (ONI)	
	Correlation	*p*	Correlation	*p*
Named storms	−0.12	0.45	−0.36	0.02
Named storm days	−0.21	0.19	−0.34	0.03
Hurricanes	−0.27	0.09	−0.48	0.001
Hurricane days	−0.32	0.04	−0.43	0.01
Major Hurricanes	−0.32	0.04	−0.39	0.01
Major Hurricane days	−0.32	0.04	−0.31	0.05
ACE	−0.3	0.05	−0.4	0.01

The correlations shown in Figure 3c with the CAM onset date variations indicate significant negative correlations with Atlantic TC activity, which is largely in the western Atlantic region, through and north of the Leeward Islands, and in the

TABLE 3 | Partial correlations of basin-wide tropical cyclone metrics for the northern tropical eastern Pacific Ocean.

Basin-wide metric	CAM onset date variations		ENSO variations (ONI)	
	Correlation	*p*	Correlation	*p*
Named storms	0.5	0.001	0.45	0.003
Named storm days	0.44	0.004	0.37	0.02
Hurricanes	0.41	0.01	0.38	0.01
Hurricane days	0.35	0.02	0.32	0.04
Major Hurricanes	0.36	0.02	0.43	0.01
Major Hurricane days	0.25	0.11	0.41	0.01
ACE	0.36	0.02	0.41	0.01

Bay of Campeche in the Gulf of Mexico. These negative correlations with the CAM onset are linked to an early or later onset, leading to higher or lower TNA TC activity respectively. In addition, the significant correlations in Figure 3c are relatively sparse in the Caribbean region compared to those in Figure 3b. However, the region of significant positive correlations (implying later or early onset of CAM leads to more or less TC activity) over the TEP in Figure 3c is more spatially extensive in the open ocean away from the coast compared to Figure 3b.

The partial correlations of TNA TC activity with ONI and CAM onset date variability indicate that the teleconnections are comparable between the two indices. For instance, the correlations in Table 2 of onset date of the CAM and ONI with hurricane days is −0.32 and −0.43, major hurricanes (TCs with sustained wind speeds 111 mph or 178 km/h) is −0.32 and −0.39, major hurricane days is −0.32 and −0.31 and Accumulated Cyclone Energy (ACE) is −0.3 and −0.4 respectively. However, the correlations of onset date variations of CAM are weak and insignificant for named storms, named storm days and hurricanes in the TNA while it is relatively stronger and statistically significant with ONI (Table 2).

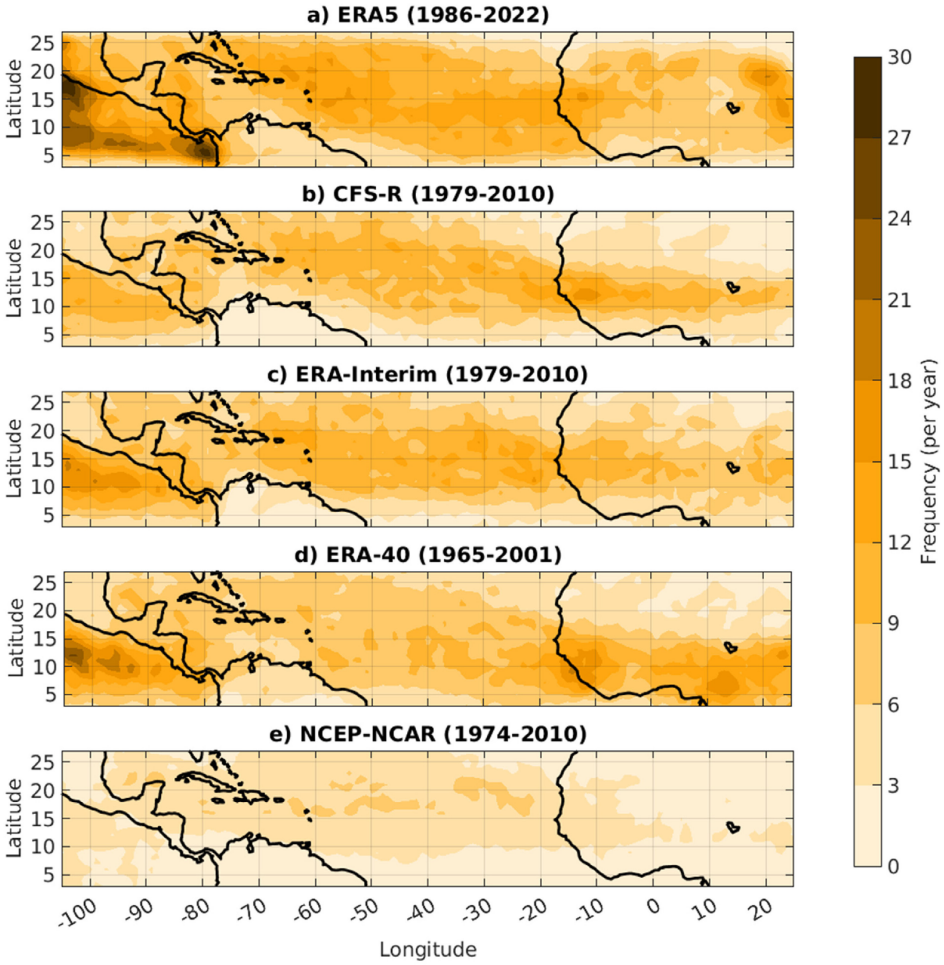

FIGURE 4 | The climatological track density of tropical easterly waves at 600 hPa from May to November in (a) ERA5, (b) CFS-R, (c) ERA-Interim, (d) ERA-40 and (e) NCEP-NCAR. The years used in computing the climatology are indicated in the title of each panel. [Colour figure can be viewed at wileyonlinelibrary.com]

The partial correlations of TEP TC activity in Table 3 also show a comparable and strong relationship with both ONI and CAM onset date variations. An exception, however, is the weak and insignificant correlation of major hurricane days with onset date variations of CAM (Table 3). These relationships in Tables 2 and 3 have practical significance as CAM onset date variations, which typically occur in late April or May, precede the TC activity in both ocean basins by a couple of weeks to a month, and it also supplements the teleconnections with ONI (as will be illustrated and explained later in the paper). It may be noted that the CAM onset date variations are slightly more strongly correlated with most of the basin-wide TC metrics over the TEP in Table 3 than with the corresponding metrics in the TNA in Table 2. However, the ENSO teleconnections with the basin-wide TC metrics are comparable in the two ocean basins.

3.3 | Relation With Tropical Easterly Wave Activity

As pointed out in Section 2, the TEWs are diagnosed at 600 hPa in five different global atmospheric reanalysis datasets (Figure 4). There are significant differences in the track densities of the TEWs across these five atmospheric reanalyses over the TNA and TEP. Figure 4a shows that ERA5 produces more TEWs in the east Pacific than other reanalyses, extending from the Panama Bight region in the east to west of 100° W. Likewise, ERA-40 in Figure 4d shows comparatively weaker TEW activity in the tropical Atlantic but higher TEW activity over the TEP than most other reanalyses with the exception of NCEP-NCAR and ERA5. CFS-R in Figure S1b and ERA-Interim in Figure 4c show comparable TEW activity in the two ocean basins. Belanger et al. (2017) similarly noted a higher density of TEWs in the eastern Pacific basin relative to the Caribbean Sea. Many studies point out that in situ generation of TEWs in the TEP is a dominant feature in addition to their translation across the Atlantic from West Africa (Serra et al. 2008; Toma and Webster 2010a, 2010b; Rydbeck et al. 2017; DeLaune et al. 2025). In contrast, Figure 4e shows that NCEP-NCAR has relatively far less TEW activity in both the TNA and TEP basins relative to other reanalyses. Similarly, the five reanalyses show large diversity in the track density of TEWs over northern Africa (Figure 4).

The correlations of the ONI with TEW track density in Figure 5 show significant negative correlations, which consistently appear in the Caribbean region and over continental regions of the Americas west of 50° W and roughly between the latitudes

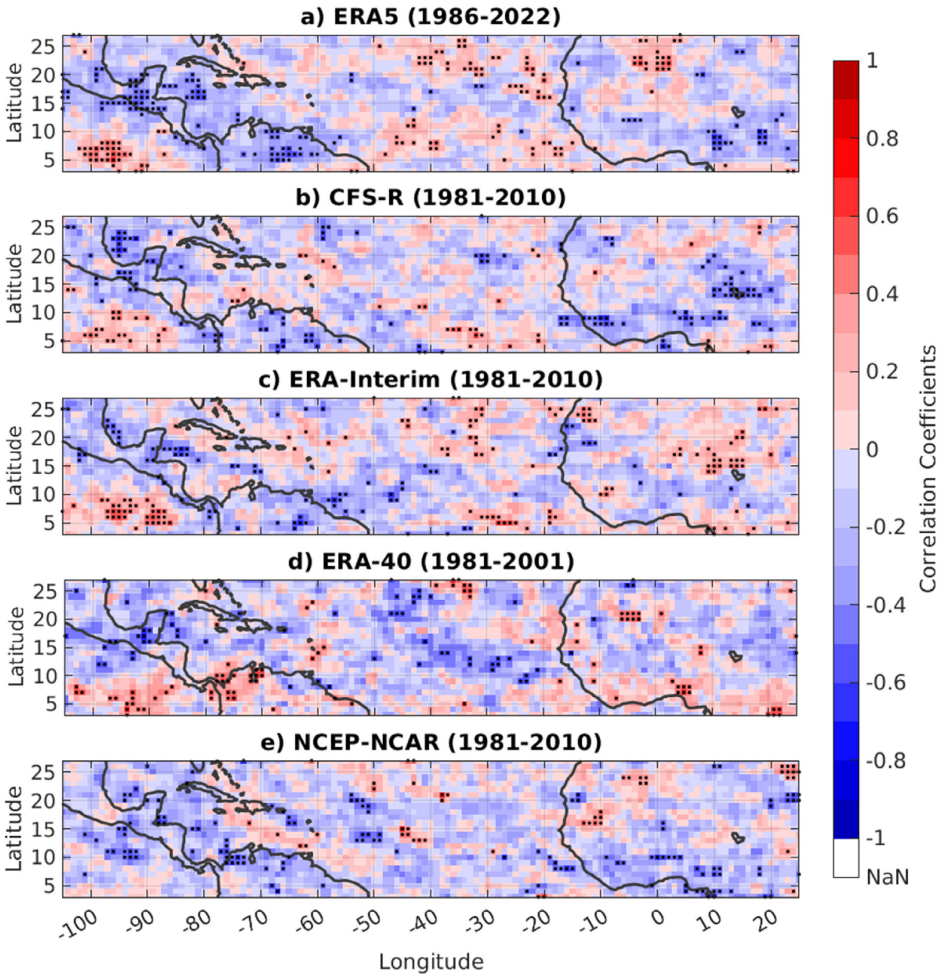

FIGURE 5 | The partial correlations of the track density of all May-to-November tropical easterly waves (TEWs) at 600 hPa in (a) ERA5, (b) CFS-R, (c) ERA-Interim, (d) ERA-40 and (e) NCEP-NCAR reanalysis with contemporaneous May-to-November averaged Oceanic Niño Index (ONI). The stippled values signify statistical significance at 5% significance level according to t-test. [Colour figure can be viewed at wileyonlinelibrary.com]

of 5° N and 20° N with significant positive correlations over the open TEP, west of ~85° W. This relationship of the ONI index with the TEW activity broadly coincides with its relationship with the named TC activity shown in Figure 3b that exhibited negative correlations over the Caribbean region and positive correlation in the TEP. The correlations exhibited by NCEP-NCAR reanalysis over the TEP in Figure 5e, however, are not consistent with the other reanalyses, which is not surprising given its under-reported TEWs (Figure 4e). Furthermore, the correlations between ONI and TEW track density in the rest of the regions outside of the Caribbean Sea and TEP are not consistent across the reanalyses and are spatially not as coherent (Figure 5).

The correlations of the onset date variations of CAM with track density of TEWs in Figure 6 show a relatively consistent negative correlation across the five reanalyses over the western Atlantic Ocean, Bay of Campeche and over the Caribbean Sea, which is broadly coincident with similar correlations with named TCs in Figure 2c. In other words, early or later onset of the CAM is likely to be associated with higher or lower TEWs in regions with negative correlations in Figure 6 respectively. Over the TEP, the correlations are positive in ERA5, CFSR and ERA-Interim but appear weaker and interspersed with negative correlations in ERA-40 and NCEP-NCAR reanalyses. Many of the earlier studies have suggested that the diabatic heat release from convection in the Panama Bight region can generate in situ TEWs in the TEP (e.g., Rydbeck et al. 2017; DeLaune et al. 2025). Seasonally, convection in the Panama Bight region is most active during the CAM season (Gonzalez et al. 2025). However, the appearance of the positive correlations in the TEP (in Figure 6) suggests that an early or later onset of CAM seasons is associated with less or more TEW activity respectively. This positive correlation could be suggestive of the CAM interfering with the progression of the TNA TEWs into the TEP. In the following sub-section, we will show the potential influence of the CAM on vertical shear, which could explain some of these observed facts. It may be noted that the correlations in Figures 5 and 6 are similar, suggesting the compounding influence of CAM and ENSO variations on TEWs.

3.4 | Teleconnections With the Large-Scale Variables

The May-to-November averaged ONI index has a well-known association with the North Atlantic Subtropical High (NASH; Figure 7a), mid-level (700 hPa) relative humidity (Figure 7b),

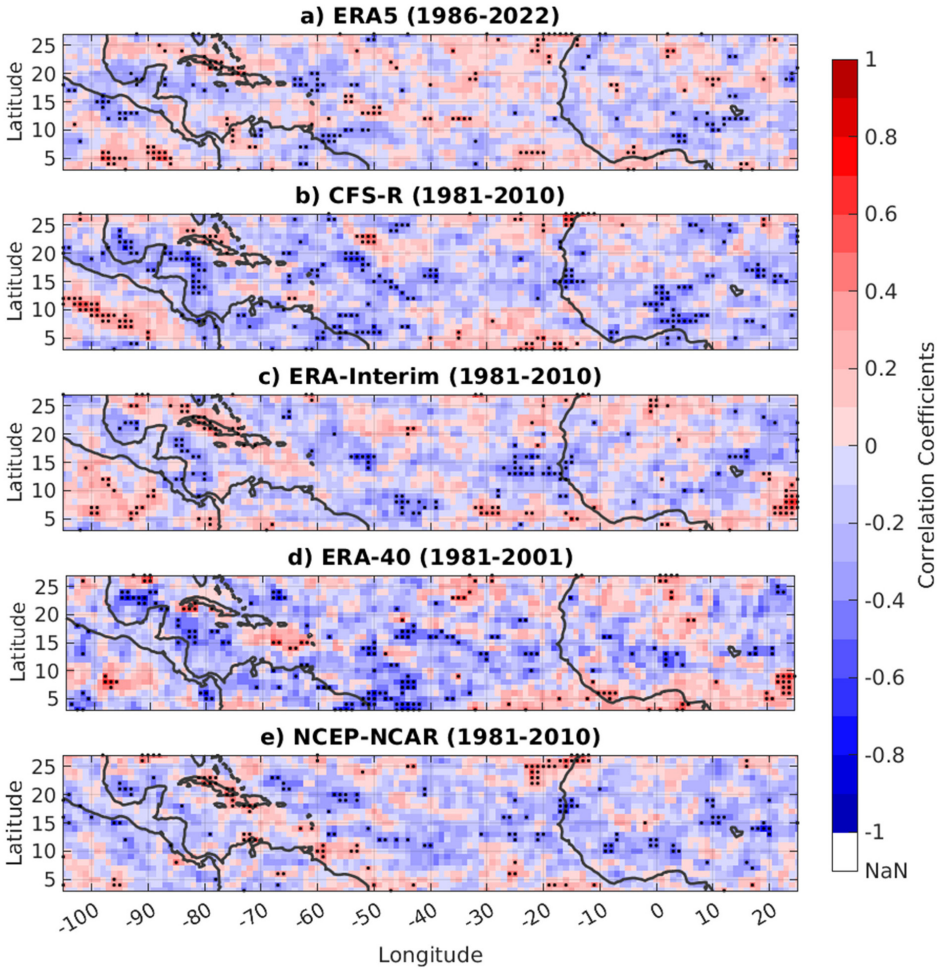

FIGURE 6 | The partial correlations of the track density of all May-to-November tropical easterly waves at 600 hPa in (a) ERA5, (b) CFS-R, (c) ERA-Interim, (d) ERA-40 and (e) NCEP-NCAR reanalysis with Central American Monsoon onset dates. The stippled values signify statistical significance at 5% significance level according to t-test. [Colour figure can be viewed at wileyonlinelibrary.com]

bulk vertical shear (Figure 7c) and sea surface temperature (Figure 7d; Gray 1984; Goldenberg and Shapiro 1996; Enfield and Mayer 1997; Li et al. 2012; Colbert and Soden 2012). The correlations in Figure 7a suggest that with positive (El Niño) or negative (La Niña) ONI conditions, the NASH strengthens (higher 850 hPa gpm) or weakens (lower 850 hPa gpm) respectively. This is also illustrated from the composites of 850 hPa geopotential height anomalies shown in Figure S1. Like other studies, Figures 7a and S1 also suggest that NASH is located further eastward or is strengthened eastward during El Niño summers. On the other hand, in the TEP, ONI teleconnections with the 850 hPa height variations are contrary to those over the TNA (Figure 7a), with 850 hPa heights reducing or increasing during positive (El Niño) or negative (La Niña) phases of ONI respectively. Similarly, the correlations in Figure 7b show that mid-level relative humidity at 700 hPa decreases or increases in the Caribbean Sea and in the TEP under El Niño or La Niña conditions respectively.

The westerly vertical wind shear in the tropical western Atlantic and in the Caribbean region increases or decreases with positive or negative ONI (Figure 7c) respectively. The impact of ENSO on the wind shear over the western Atlantic can be assessed from the corresponding wind composite anomalies at 200 hPa (Figure S2) and at 850 hPa (Figure S3). This enhancement of westerly wind shear can be further understood from Figures S2b and S3b, which show the increase in the westerly wind anomalies at 200 hPa and easterly wind anomalies at 850 hPa over the western Atlantic during El Niño seasons respectively. Likewise, the easterly wind shear in the TEP decreases or increases with positive or negative ONI (Figure 7c) respectively. These changes in the vertical shear over TEP are associated with the corresponding appearance of westerly wind anomalies at 200 hPa (Figure S2b) and lower-level easterly anomalies (Figure S3b) during El Niño seasons. May-to-November ONI has a strong relationship with the corresponding SST anomalies only in the TEP (Figure 7d), which essentially reflects El Niño or La Niña conditions with positive or negative ONI respectively. These relationships in Figure 7a–d are consistent with well-known ENSO teleconnections on TC variations of the western hemisphere (e.g., Balaguru et al. 2013; Bell and Chelliah 2006; Camargo et al. 2008; Gray 1984; Klotzbach 2007, 2011).

The corresponding partial correlations of the onset date variations of CAM with these large-scale variables are shown in Figure 8. Generally, the correlations in Figure 8 are comparable to those with ONI in Figure 7, with slightly weaker magnitudes and are less spatially extensive. Furthermore, the ONI has a stronger relationship with some of these large-scale variables over the continental regions of North Africa (Figure 7) that is largely absent with onset date variations of CAM (Figure 8). The modulation of the NASH by onset date variations of the CAM in Figure 8a indicates essentially the association of the variations of the NASH with CAM seasonal rainfall, with the latter being a wetter or a drier season in an earlier or later onset season, from a weaker or a stronger NASH respectively. In comparing Figure S1d,e, it can be clearly seen that NASH is weaker in early than late onset CAM

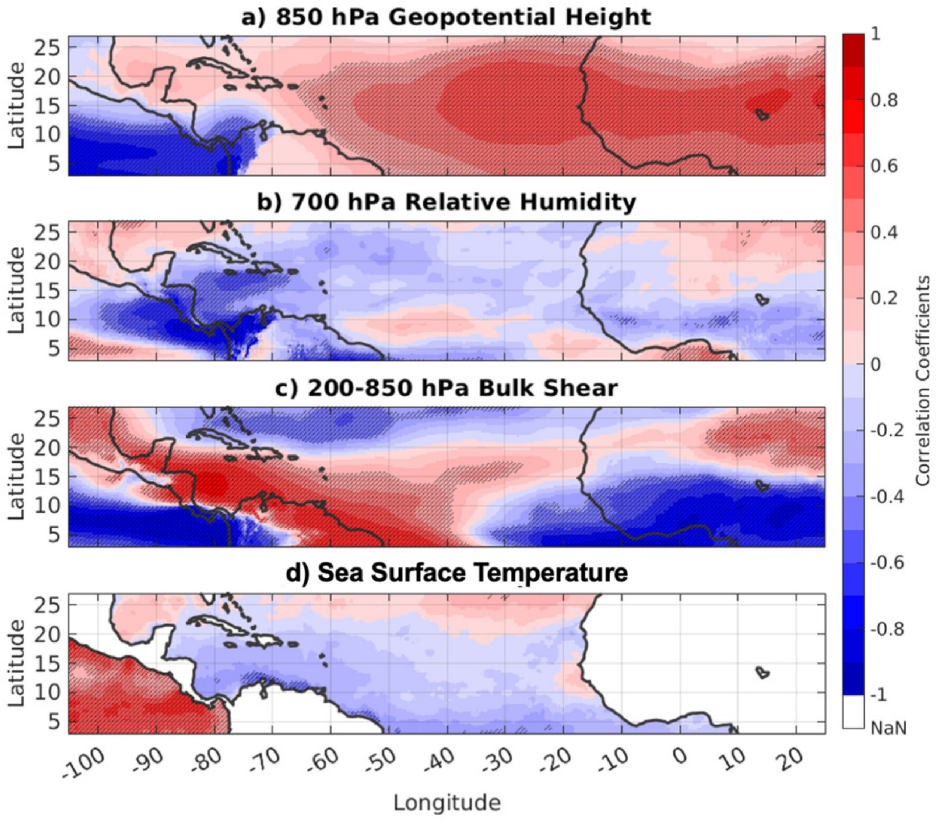

FIGURE 7 | The partial correlations of May to November Oceanic Niño Index (ONI) with corresponding May to November mean (a) 850 hPa geopotential height, (b) 700 hPa relative humidity, (c) 200–850 hPa bulk shear from ERA5 and (d) SST anomalies from OISSTv2. The significant values at 5% significance level according to *t*-test are indicated by slanted lines. [Colour figure can be viewed at wileyonlinelibrary.com]

seasons. Misra et al. (2014) point out that a weakened or a strengthened NASH associated with weaker or enhanced trade wind easterlies enhances or reduces the moisture flux convergence over the Central American isthmus resulting in a wetter or a drier CAM season respectively. It may be noted that the changes in NASH between early and late onset CAM seasons are larger than positive or negative ONI seasons (Figure S1). Similarly, mid-level (700 hPa) relative humidity in the Caribbean region and TEP is enhanced or reduced from earlier or later onset of the season, which is related to a wetter or a drier CAM season (Figure 5b) respectively. The correlations with the vertical shear in Figure 8c, indicate that the westerly vertical wind shear is decreased or increased in the Caribbean region, while the prevalent easterly shear in the TEP is raised or reduced with early or later onset of the CAM season respectively. The composite of the 200 hPa wind anomalies in Figure S2d for early onset CAM seasons clearly shows easterly wind anomalies over the western Atlantic and over TEP, with the corresponding appearance of westerly wind anomalies at 850 hPa in the western Atlantic and in the TEP in Figure S3d.

3.5 | TC Activity Relations With CAM Onset Date and ONI Variations

We now reexamine the May-to-November TC track density variations as composite anomalies for the various combinations of ENSO phases and variations of CAM in this sub-section. Figure 9a shows the composite TC track density for La Niña years, which indicates an excess of them in the western TNA, eastern Caribbean and in the western Gulf of Mexico. However, for a combination of La Niña and early onset of CAM seasons, we observe that the significant positive anomalies in the TNA are further enhanced in Figure 9b relative to Figure 9a. For instance, more TCs form in the western TNA, Caribbean Sea and the Bay of Campeche (Figure 9b). In contrast, for La Niña and late onset of the CAM seasons, the strongest positive anomalies are observed in the far eastern TNA and southwestern Caribbean Sea (Figure 9c). However, at the same time, we also observe fewer TCs in the Bay of Campeche and western TNA (west of 50° W) in Figure 9c relative to Figure 9a,b. It may be noted that in the TEP there are insignificant TC anomalies for La Niña seasons (Figure 9a), with slightly enhanced TC anomalies for La Niña and early onset of CAM seasons just off the southern Pacific coast of Mexico (Figure 9b), which gets diminished to insignificant anomalies for La Niña and late onset of CAM seasons (Figure 9c).

In contrast, the TC anomalies are largely insignificant for El Niño seasons in Figure 9d over both tropical ocean basins except in a small region west of 100° W, which shows a southward shift of increased TC activity around 15° N. The TC anomalies in the TEP are largely similar for El Niño and early onset of CAM seasons (Figure 9e) compared to the El Niño seasons (Figure 9d), although there is a slight enhancement of TC anomalies in the Gulf of Tehuantepec. In Figure 9f, for El Niño and late onset of CAM seasons, the southward shift of the TC anomalies across 15° N and west of 100° W is slightly enhanced compared to Figure 9d,e.

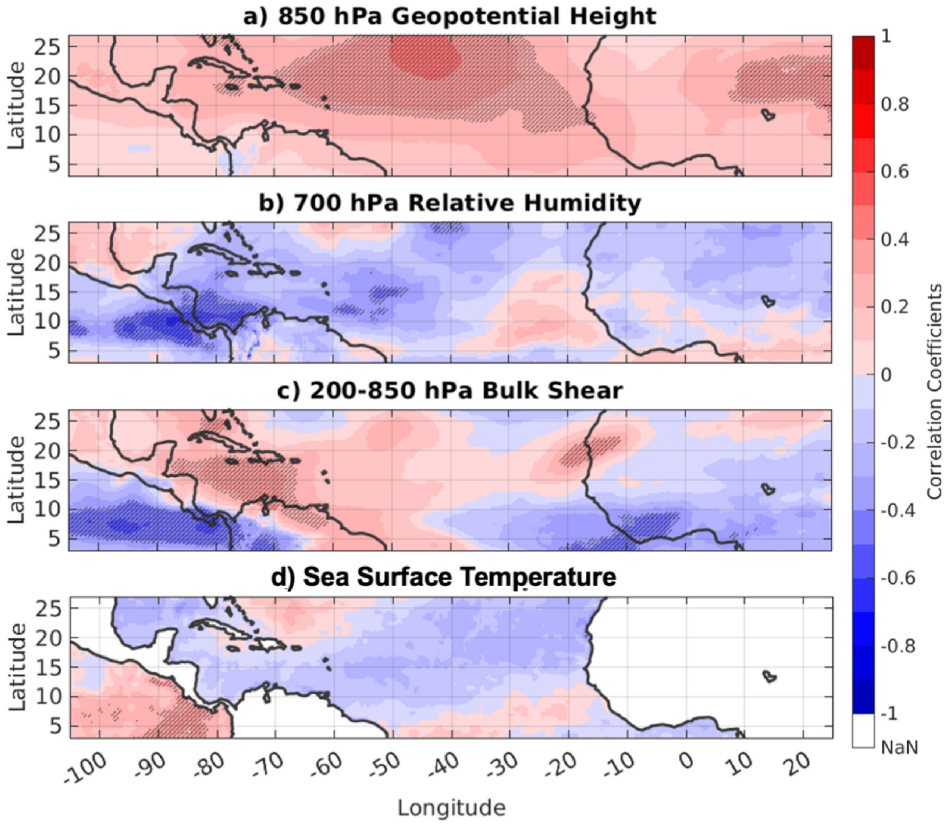

FIGURE 8 | The partial correlations of the onset date of the Central American Monsoon (CAM) with the May to November mean (a) 850 hPa geopotential height, (b) 700 hPa relative humidity, (c) magnitude of (200–850 hPa) bulk shear from ERA5 and (d) SST anomalies from OISSTv2. The significant values at 5% significance level according to t-test are indicated by slanted lines. [Colour figure can be viewed at wileyonlinelibrary.com]

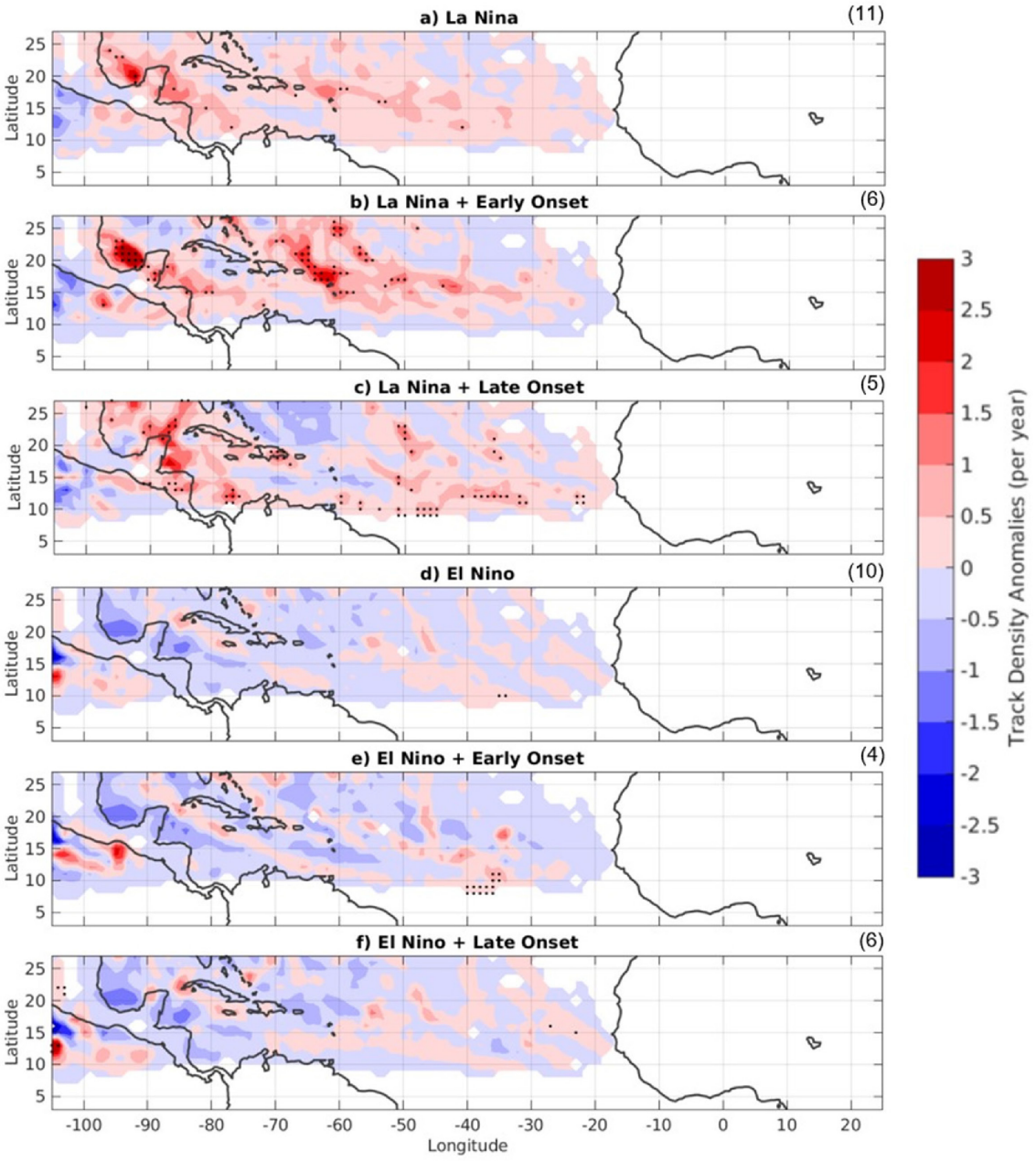

FIGURE 9 | The composite May to November named TC track density anomalies for (a) La Niña, (b) La Niña and early onset of CAM seasons, (c) La Niña and late onset of CAM seasons, (d) El Niño, (e) El Niño and early onset of CAM seasons and (f) El Niño and late onset of CAM seasons. The numbers in the upper right corner of each panel indicate the number of seasons out of the 43 years used in generating the composite anomalies. The stippled values signify statistical significance at 5% significance level according to *t*-test. [Colour figure can be viewed at wileyonlinelibrary.com]

4 | Discussion and Conclusions

The teleconnection of ENSO with the seasonal TC activity in both ocean basins is well known through its influence on vertical wind shear, mid-level humidity, low-level vorticity and TEWs. This is reiterated in this study. But we also find that the onset date variations of the CAM have teleconnections with the NASH in the TNA, mid-level relative humidity and vertical wind shear over the Caribbean Sea and TEP and sea surface temperature in the TEP. We find, for instance, early onset of the CAM is associated with weakening of NASH, an increase in mid-level relative humidity across the Central American isthmus and adjacent oceans and weaker vertical wind shear across the Caribbean Sea, stronger vertical shear over the TEP and colder SST anomalies in the TEP. These teleconnections of the onset date of CAM with the large-scale variables associated with TC activity in the western hemisphere are largely a result of the robust association of the former with the seasonal rainfall anomalies of CAM shown in Rodgers et al. (2024). In terms of teleconnections with track densities of TCs, warm and cold ENSO events produce more and less TCs in the TEP respectively. In contrast, El Niño and La Niña events are associated with less and more TCs in the Caribbean and western Gulf of Mexico region respectively.

Similarly, the teleconnections of La Niña yield more TCs in the western Caribbean Sea and Gulf of Mexico. But the response of TC activity over TEP is much weaker in La Niña seasons. The onset date variations of CAM show similar modulation of TC activity in the TNA and TEP as ENSO. We find that early or late onset of CAM is related to more or less TCs in the TNA and less or more TCs in the TEP respectively.

The strongest response of increased seasonal TC activity in the western TNA, western Caribbean Sea and western Gulf of Mexico is observed when La Niña overlaps with seasons of early CAM onset. In such seasons, we find that there are more TCs forming in the western TNA, eastern Caribbean and in the western Gulf of Mexico relative to just La Niña seasons. It is also observed that overlapping La Niña and early CAM onset seasons also reinforce each other in the weakening of the westerly vertical wind shear and raising mid-level relative humidity in the western Atlantic. In contrast, the response of the seasonal TC activity over TNA is weak to insignificant during El Niño years with either early or late onset of CAM season but appears slightly significant in the TEP.

This modulation of seasonal TC activity by ENSO and variations of CAM appears to be more robust than TC density anomalies assessed at discrete grid points when basin-wide metrics like ACE, total number of TCs or number of TC days are examined. This is more a reflection of the limited sample size of TC track densities, which is significantly ameliorated in basin-wide aggregated TC statistics. We find that the variation of CAM onset date has a larger impact on the variations of basin-wide metrics of hurricanes and major hurricanes in both the TNA and TEP compared to basin-wide metrics associated with just tropical storms. In contrast, ENSO has an impact on basin-wide metrics for all TCs in both basins. From the analysis of the basin-wide statistics of the TCs, it is clear that in seasons when La Niña and early onset of the CAM coincide, the enhancement of the TC activity in the TNA is more likely than in other seasons, as the signals from the two sources are likely to reinforce each other. This stems from similar teleconnections that yield weaker NASH, and increased mid-level relative humidity, reduced vertical wind shear and increased TEW activity in the Caribbean region. In the TEP, however, the coincidence of El Niño with the late onset of CAM is likely to yield an active TC season from warmer in situ SSTs and reduced vertical wind shear. Similarly, our analysis suggests that La Niña and early onset of the CAM are likely to produce a suppressed TC activity in the TEP.

The study highlights an important source of modulation of seasonal TC activity in the western hemisphere by the CAM onset date variations. This supplements the existing teleconnection of ENSO variations with seasonal TC activity in the western hemisphere. However, variations in CAM onset have relatively weak correlations with the ENSO variations, which suggests that they offer an independent source of modulation of the seasonal TC activity in the western hemisphere. Furthermore, the onset date variations of CAM offer a predictive value to the seasonal TC and TEW activity by appearing in advance or nearly at the start of the TC season in the western hemisphere. Therefore, we believe exploring leveraging the onset date variations of the CAM with the much-improved seasonal ENSO prediction skills from the current climate models could yield more beneficial seasonal prediction skills of TC activity in the western hemisphere.

Author Contributions

Connor DeLaune: conceptualisation, methodology, software, validation, formal analysis, investigation, resources, data curation, visualisation, review and editing. **Vasubandhu Misra:** writing original draft, review and editing. **C. B. Jayasankar:** review and editing, data acquisition, data curation, formal analysis.

Acknowledgements

We acknowledge the support from the NASA grant 80NSSC22K0595.

Funding

This work was supported by the National Aeronautics and Space Administration (80NSSC22K0595).

Conflicts of Interest

The authors declare no conflicts of interest.

Data Availability Statement

The upper air ERA5 reanalysis data were obtained from https://www.ecmwf.int/en/forecasts/datasets/reanalysis-datasets/era5. The tropical easterly wave tracking algorithm follows Belanger et al. (2017) and is available from ftp://ftp.ncdc.noaa.gov/pub/data/aewc-v1/src/src_readme.docx. The upper air NCEP-NCAR data are available from https://psl.noaa.gov/data/gridded/data.ncep.reanalysis.html. The upper air CFSR data are available from https://www.ncei.noaa.gov/access/metadata/landing-page/bin/iso?id=gov.noaa.ncdc:C00766. The upper air ERA-Interim data are available from https://catalogue.ceda.ac.uk/uuid/30bf1d10579c4812800f2daaae951a68/. The upper air ERA-40 data are available from https://catalogue.ceda.ac.uk/uuid/e53d40669b5848cb86b4a9bcda29467e. The OISSTv2 data are available from https://www.ncei.noaa.gov/products/optimum-interpolation-sst. The CHIRPS daily rainfall data are available from https://data.chc.ucsb.edu/products/CHIRPS-2.0/global_daily/.

References

Amador, J. A. 2008. "The Intra-Americas Sea Low-Level Jet: Overview and Future Research." *Annals of the New York Academy of Sciences* 1146: 153–188.

Amador, J. A., E. R. Rivera, A. M. Durán-Quesada, et al. 2016. "The Easternmost Tropical Pacific. Part I: A Climate Review." *Revista de Biología Tropical* 64, no. S1: 1–22. https://doi.org/10.15517/rbt.v64i1.23407.

Balaguru, K., R. L. Leung, and J.-H. Yoon. 2013. "Oceanic Control of Northeast Pacific Hurricane Activity at Interannual Timescales." *Environmental Research Letters* 8: 044009.

Barnston, A. G., M. Chelliah, and S. B. Goldenberg. 1997. "Documentation of a Highly ENSO-Related Sst Region in the Equatorial Pacific: Research Note." *Atmosphere-Ocean* 35: 367–383.

Belanger, J. I., M. T. Jelinek, and J. A. Curry. 2017. "A Climatology of Easterly Waves in the Tropical Western Hemisphere." *Geoscience Data Journal* 3: 40–49. https://doi.org/10.1002/gdj3.40.

Bell, G. D., and M. Chelliah. 2006. "Leading Tropical Modes Associated With Interannual and Multidecadal Fluctuations in North Atlantic Hurricane Activity." *Journal of Climate* 19: 590–612.

Camargo, S. J., and A. H. Sobel. 2005. "Western North Pacific Tropical Cyclone Intensity and ENSO." *Journal of Climate* 18, no. 15: 2996–3006.

Camargo, S. J., A. H. Sobel, A. G. Barnston, and M. Ghil. 2008. "Clustering of Eastern North Pacific Tropical Cyclone Tracks: ENSO and MJO Effects." *Geochemistry, Geophysics, Geosystems* 9: 5.

Colbert, A. J., and B. J. Soden. 2012. "Climatological Variations in North Atlantic Tropical Cyclone Tracks." *Journal of Climate* 25: 657–673.

Collins, J. M. 2007. "El Niño and La Niña Induced Changes in Eastern Pacific Hurricane Tracks." *Journal of Climate* 20, no. 9: 1407–1424.

Colorado State University. 2025. "CSU Tropical Cyclones, Radar, Atmospheric Modeling, and Software Team (TC-RAMS)." https://tropical.colostate.edu/archive.html.

Dee, D. P., and Coauthors. 2011. "The ERA-Interim Reanalysis: Configuration and Performance of the Data Assimilation System." *Quart. J. Roy. Meteor. Soc* 137, no. 656: 553–597.

DeLaune, C., V. Misra, and C. B. Jayasankar, 2025. "Impact of Dynamic Downscaling on the Simulation of Tropical Easterly Waves in the Intra-Americas Seas." *Journal of Geophysical Research (Atmospheres)* 130: e2025JD043454. https://doi.org/10.1029/2025JD043454.

Durán-Quesada, A. M., L. Gimeno, and J. Amador. 2017. "Role of Moisture Transport for Central American Precipitation." *Earth System Dynamics* 8: 147–161. https://doi.org/10.5194/esd-8-147-2017.

Durán-Quesada, A. M., R. Sori, P. Ordonez, and L. Gimeno. 2020. "Climate Perspectives in the Intra-Americas Seas." *Atmosphere* 11, no. 9: 959. https://doi.org/10.3390/atmos11090959.

Enfield, D., and E. Alfaro. 1999. "The Dependence of Caribbean Rainfall on the Interaction of the Tropical Atlantic and Pacific Oceans." *Journal of Climate* 12: 2093–2103. https://doi.org/10.1175/1520-0442(1999)012<2093:TDOCRO>2.0.CO;2.

Enfield, D. B., and D. A. Mayer. 1997. "Tropical Atlantic SST Variability and Its Relation to El Niño–Southern Oscillation." *Journal of Geophysical Research* 102, no. C1: 929–945.

Frank, W. M., and G. S. Young. 2007. "The Interannual Variability of Eastern North Pacific Tropical Cyclones." *Monthly Weather Review* 135, no. 4: 1405–1419.

Funk, C., P. Peterson, M. Landsfeld, et al. 2015. "The Climate Hazards Infrared Precipitation With Stations: A New Environmental Record for Monitoring Extremes." *Scientific Data* 2: 150066. https://doi.org/10.1038/sdata.2015.66.

Giannini, A., Y. Kushnir, and M. A. Cane. 2000. "Interannual Variability of Caribbean Rainfall, ENSO, and the Atlantic Ocean." *Journal of Climate* 13: 297–311.

Goldenberg, S. B., C. W. Landsea, A. M. Mestas-Nuñez, and W. M. Gray. 2001. "The Recent Increase in Atlantic Hurricane Activity: Causes and Implications." *Science* 293: 474–479.

Goldenberg, S. B., and L. J. Shapiro. 1996. "Physical Mechanisms for the Association of El Niño and West African Rainfall With Atlantic Major Hurricane Activity." *Journal of Climate* 9: 1169–1187.

Gonzalez, J., V. Misra, and C. B. Jayasankar. 2025. "The Impact of Cumulus Parameterization on Regional Climate Simulations of Central American Climate." *J. Appl. Meteo. And Climatol* 64: 1629–1649. https://doi.org/10.1175/JAMC-D-24-0240.1.

Gray, W. M. 1984. "Atlantic Seasonal Hurricane Frequency. Part I: El Niño and 30 Mb Quasi-Biennial Oscillation Influences." *Monthly Weather Review* 112: 1649–1668.

Hersbach, H., W. Bell, P. Berrisford, et al. 2020. "The ERA5 Global Reanalysis." *Quarterly Journal of the Royal Meteorological Society* 146, no. 730: 1999–2049. https://doi.org/10.1002/qj.3803.

Huang, B., C. Liu, V. Banzon, et al. 2021. "Improvements of the Daily Optimum Interpolation Sea Surface Temperature (DOISST) Version 2.1." *Journal of Climate* 34: 2923–2939. https://doi.org/10.1175/JCLI-D-20-0166.1.

Huang, B., P. W. Thorne, V. F. Banzon, et al. 2017. "Extended Reconstructed Sea Surface Temperature, Version 5 (ERSSTv5): Upgrades, Validations, and Intercomparisons." *Journal of Climate* 30: 8179–8205.

Kalnay, E., and Coauthors. 1996. "The NCEP/NCAR 40-Year Reanalysis Project." *Bull. Amer. Meteor. Soc* 77: 437–471.

Klotzbach, P. J. 2007. "Recent Developments in Statistical Prediction of Seasonal Atlantic Basin Tropical Cyclone Activity." *Tellus* 59: 511–518.

Klotzbach, P. J. 2011. "The Influence of El Niño–Southern Oscillation and the Atlantic Multidecadal Oscillation on Caribbean Tropical Cyclone Activity." *Journal of Climate* 24: 721–731.

Landsea, C. W., and J. L. Franklin. 2013. "Atlantic Hurricane Database Uncertainty and Presentation of a New Database Format." *Monthly Weather Review* 141: 3576–3592.

Li, W., L. Li, R. Fu, Y. Deng, and H. Wang. 2012. "Changes to the North Atlantic Subtropical High and Its Role in the Intensification of Summer Rainfall Variability in the Southeastern United States." *Journal of Climate* 25: 149–164.

Misra, V., H. Li, and M. Kozar. 2014. "The Precursors in the Intra-Americas Seas to Seasonal Climate Variations Over North America." *Journal of Geophysical Research, Oceans* 119, no. 5: 2938–2948. https://doi.org/10.1002/2014JC009911.

Radok, U., and T. J. Brown. 1993. "Anomaly Correlation and Alternative: Partial Correlation." *Monthly Weather Review* 121: 1269–1271. https://doi.org/10.1175/1520-0493(1993)121<1269:ACAAAP>2.0CO;2.

Reynolds, R. W., T. M. Smith, C. Liu, D. B. Chelton, K. S. Casey, and M. G. Schlax. 2007. "Daily High-Resolution-Blended Analyses for Sea Surface Temperature." *Journal of Climate* 20: 5473–5496.

Rodgers, J., V. Misra, and C. B. Jayasankar. 2024. "Using the Observed Variations of the Start Date of the Rainy Season Over Central America for Its Reliable Seasonal Outlook." *Journal of Climate* 37: 4901–4913.

Ruti, P. M., and A. Dell'Aquila. 2010. "The Twentieth Century African Easterly Waves in Reanalysis Systems and IPCC Simulations, From Intra-Seasonal to Inter-Annual Variability." *Climate Dynamics* 35: 1099–1117.

Rydbeck, A. V., E. D. Maloney, and G. J. Alaka Jr. 2017. "In Situ Initiation of East Pacific Easterly Waves in a Regional Model." *Journal of the Atmospheric Sciences* 74, no. 2: 333–351.

Saha, S., and Coauthors. 2010. "The NCEP Climate Forecast System Reanalysis." *Bull. Amer. Meteor. Soc* 91: 1015–1058. https://doi.org/10.1175/2010BAMS3001.1.

Serra, Y. L., G. N. Kiladis, and M. F. Cronin. 2008. "Horizontal and Vertical Structure of Easterly Waves in the Pacific ITCZ." *Journal of the Atmospheric Sciences* 65: 1266–1284. https://doi.org/10.1175/2007JAS2341.1.

Shapiro, L. J. 1987. "Month-To-Month Variability of the Atlantic Tropical Circulation and Its Relationship to Tropical Storm Formation." *Monthly Weather Review* 115: 2598–2614.

Tang, B. H., and J. D. Neelin. 2004. "ENSO Influence on Atlantic Hurricanes via Tropospheric Warming." *Geophysical Research Letters* 31, no. 24: 72. https://doi.org/10.1029/2004GL021072.

Toma, V., and P. Webster. 2010a. "Oscillations of the Intertropical Convergence Zone and the Genesis of Easterly Wavespart II: Numerical Verification." *Climate Dynamics* 34: 605–613. https://doi.org/10.1007/s00382-009-0585-9.

Toma, V., and P. Webster. 2010b. "Oscillations of the Intertropical Convergence Zone and the Genesis of Easterly Waves. Part I: Diagnostics and Theory." *Climate Dynamics* 34: 587–604. https://doi.org/10.1007/s00382-009-0584-x.

Uppala, S. M., and Coauthors. 2005. "The ERA-40 Re-Analysis." *Quart. J. Roy. Meteor. Soc* 131, no. 612: 2961–3012.

Vecchi, G. A., and B. J. Soden. 2007. "Effect of Remote Sea Surface Temperature Change on Tropical Cyclone Potential Intensity." *Nature* 450: 1066–1070. https://doi.org/10.1038/nature06423.

Vera, C., W. Higgins, J. Amador, et al. 2006. "Toward a Unified View of the American Monsoon Systems." *Journal of Climate* 19: 4977–5000. https://doi.org/10.1175/JCLI3896.1.

Waylen, P. R., M. E. Quesada, and C. N. Caviedes. 1996. "Temporal and Spatial Variability of Annual Precipitation in Costa Rica and the Southern Oscillation." *International Journal of Climatology* 16: 173–193.

Webb, E. J., and B. I. Maggi. 2022. "The Ensemble Oceanic Niño Index." *International Journal of Climatology* 10: 5321–5341. https://doi.org/10.1002/joc.7535.

Supporting Information

Additional supporting information can be found online in the Supporting Information section. **Figure S1:** (a) The climatology of 850 hPa geopotential height for May-to-November and the corresponding composite means for (b) El Niño, (c) La Niña, (d) early and (e) late onset CAM seasons. The 1520 m geopotential height is indicated by the bold black contour line to illustrate the impact on the North Atlantic Subtropical High. **Figure S2:** (a) The climatological 200 hPa wind and the corresponding composite anomalies for (b) El Niño, (c) La Niña, (d) early and (e) late onset CAM seasons and La Niña and (c, d) early and late onset CAM seasons. **Figure S3:** (a) The climatological 850 hPa wind and the corresponding composite anomalies for (b) El Niño, (c) La Niña, (d) early and (e) late onset CAM seasons and La Niña and (c, d) early and late onset CAM seasons.

Supplementary Material

The Role of the Central American Monsoon in the Seasonal Variability of the Tropical Cyclone Activity in the Western Hemisphere

Connor DeLaune[1, 2], Vasubandhu Misra[1, 2, #] and C. B. Jayasankar[2]

[1]Department of Earth, Ocean and Atmospheric Science, Florida State University, Tallahassee, Florida, U. S. A.

[2]Center for Ocean-Atmospheric Prediction Studies, Florida State University, Tallahassee, Florida, U. S. A.

Corresponding Author Email: vmisra@fsu.edu

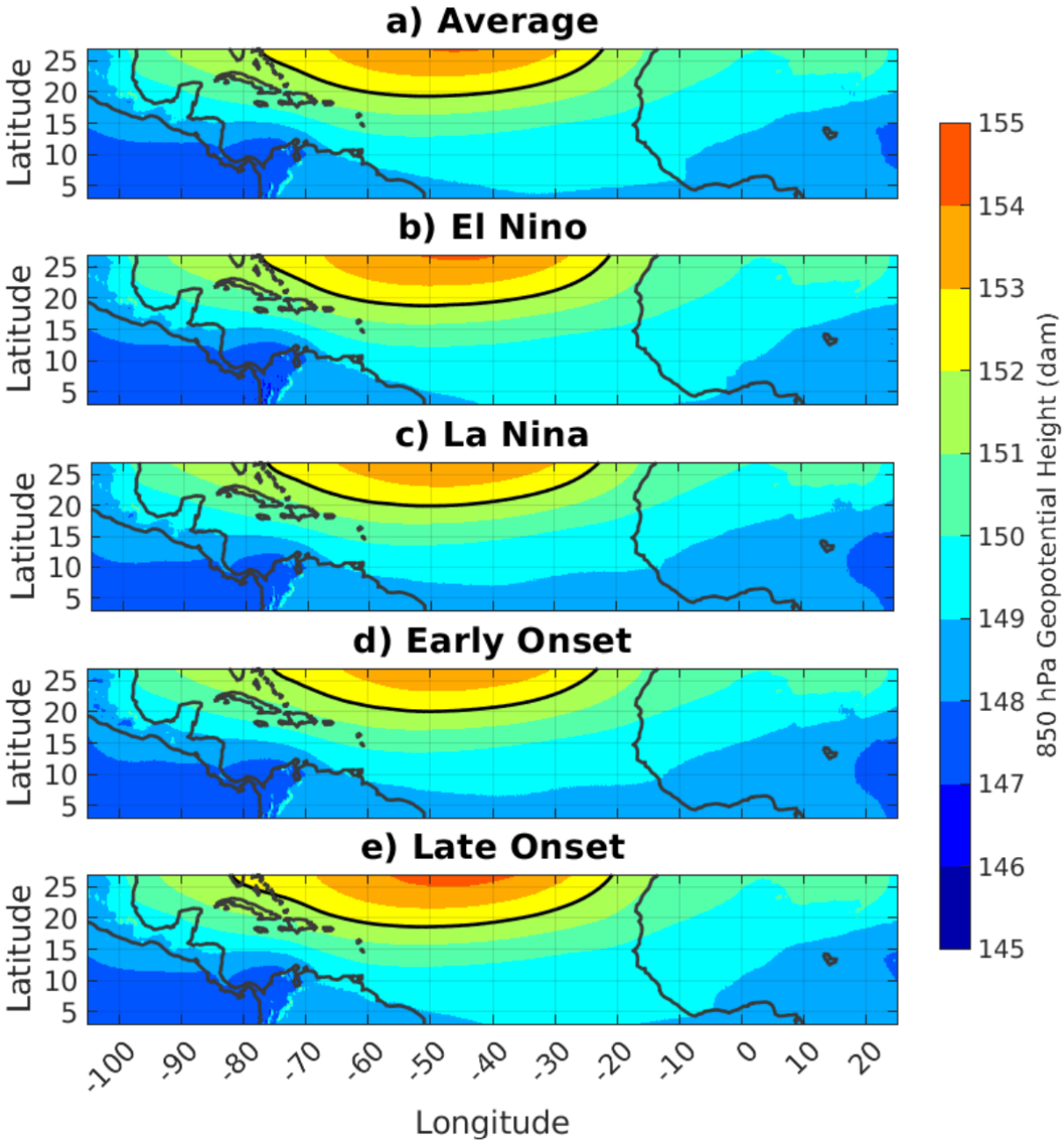

Figure S1: a) The climatology of 850hPa geopotential height for May-to-November and the corresponding composite means for b) El Niño, c) La Niña, d) early and e) late onset CAM seasons. The 1520 m geopotential height is indicated by the bold black contour line for illustrating the impact on the North Atlantic Subtropical High.

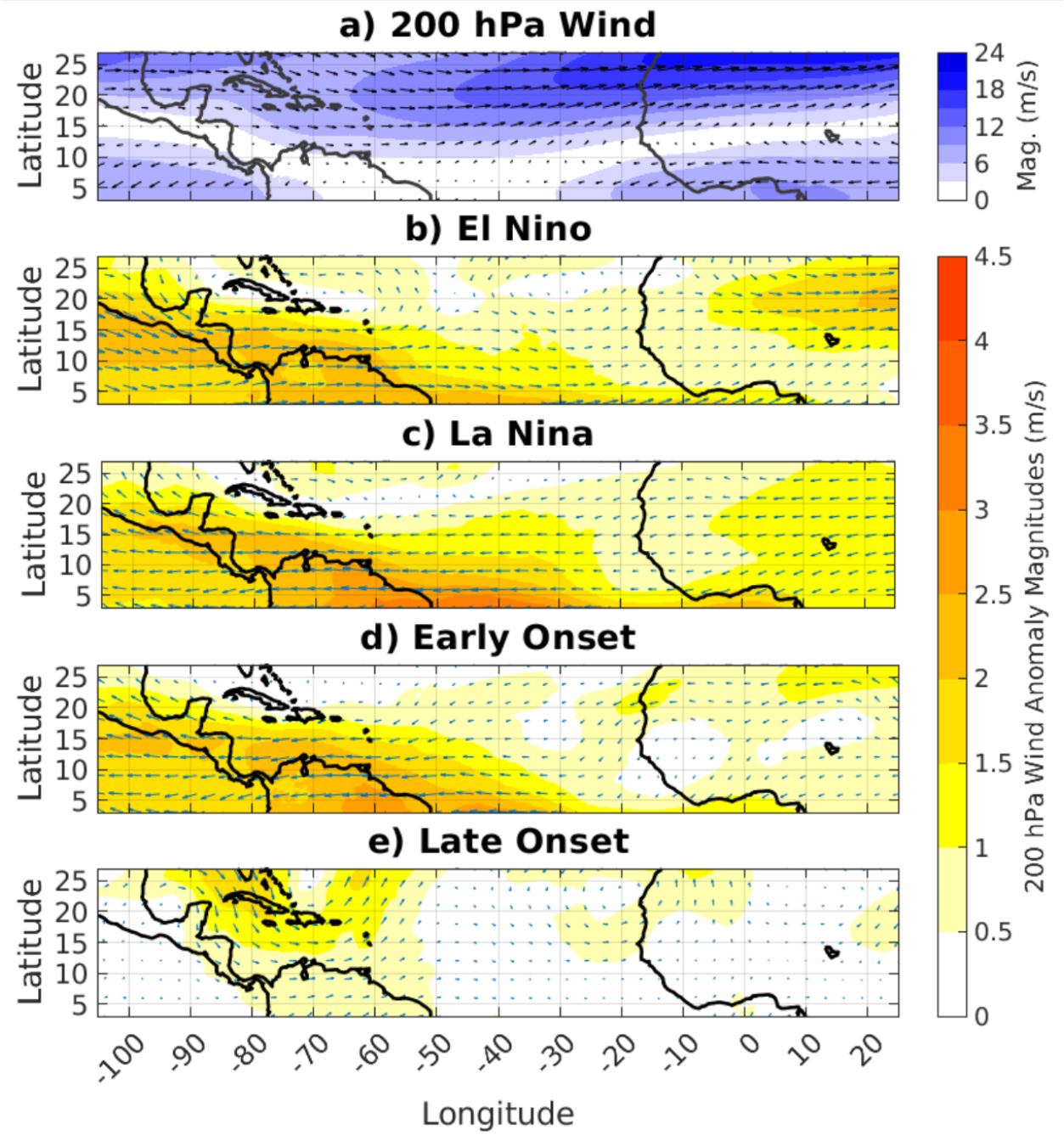

Figure S2: a) The climatological 200 hPa wind and the corresponding composite anomalies for b) El Niño, c) La Niña, d) early and e) late onset CAM seasons. and La Niña and (c, d) early and late onset CAM seasons.

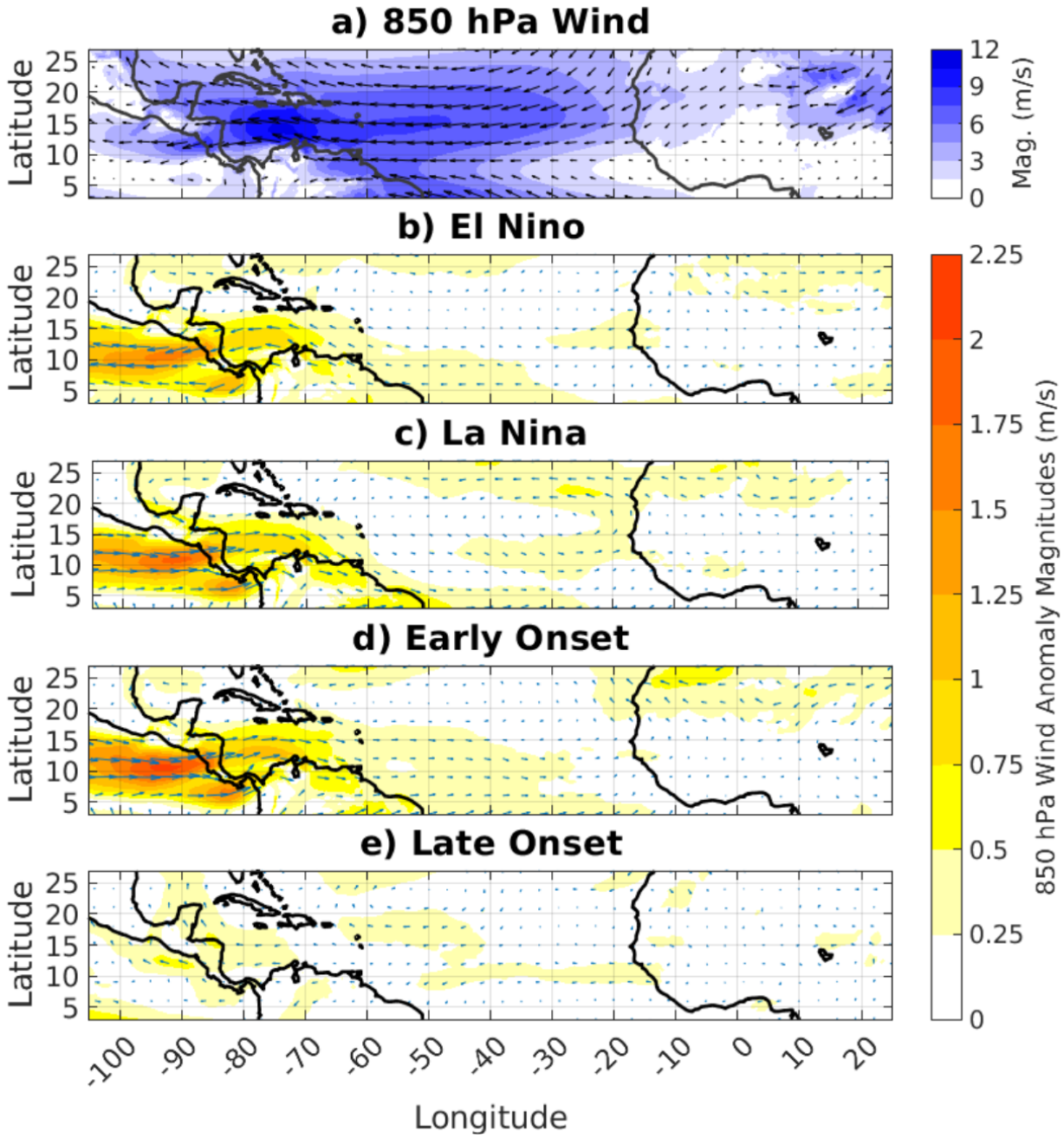

Figure S3: a) The climatological 850 hPa wind and the corresponding composite anomalies for b) El Niño, c) La Niña, d) early and e) late onset CAM seasons. and La Niña and (c, d) early and late onset CAM seasons.